

Article

A New Strategy for Dissimilar Material Joining between SiC and Al Alloys through Use of High-Si Al Alloys

Yongjing Yang¹, Ayan Bhowmik¹, Jin Lee Tan¹, Zehui Du² and Wei Zhou^{1,*} 

¹ School of Mechanical and Aerospace Engineering, Nanyang Technological University, 50 Nanyang Avenue, Singapore 639798, Singapore; yongjing001@e.ntu.edu.sg (Y.Y.); ayan99@gmail.com (A.B.); jinlee.tan@ntu.edu.sg (J.L.T.)

² Temasek Laboratories, Nanyang Technological University, 50 Nanyang Drive, Singapore 637553, Singapore; duzehui@ntu.edu.sg

* Correspondence: mwzhou@ntu.edu.sg or wzhou@cantab.net

Abstract: Joining metals and ceramics plays a crucial role in many engineering applications. The current research aims to develop a simple and convenient approach for dissimilar material joining between SiC and Al alloys. In this work, Al alloys with Si contents varying from 7 wt.% to 50 wt.% were bonded with SiC at a high temperature of 1100 °C by a pressure-less bonding process in a vacuum furnace, and shear tests were carried out to study the bonding strength. When using low-Si Al alloys to bond with SiC, the bonding strength was very low. The bonding strength of Al/SiC joints increased significantly through the use of high-Si Al alloys with 30 wt.% and 50 wt.% Si. The shear strength achieved (28.8 MPa) is far higher than those reported previously. The remarkable improvement in bonding strength is attributed to the suppression of brittle interfacial products and reduced thermal stresses. This research provides a new strategy for joining between SiC and a wide range of Al alloys through the use of high-Si Al alloys as the interlayers.

Keywords: Al-ceramic joining; dissimilar material joining; high-Si Al alloy; interfacial reaction; bonding strength



Citation: Yang, Y.; Bhowmik, A.; Tan, J.L.; Du, Z.; Zhou, W. A New Strategy for Dissimilar Material Joining between SiC and Al Alloys through Use of High-Si Al Alloys. *Metals* **2022**, *12*, 887. <https://doi.org/10.3390/met12050887>

Academic Editor: Milan Brandt

Received: 27 April 2022

Accepted: 20 May 2022

Published: 23 May 2022

Publisher's Note: MDPI stays neutral with regard to jurisdictional claims in published maps and institutional affiliations.



Copyright: © 2022 by the authors. Licensee MDPI, Basel, Switzerland. This article is an open access article distributed under the terms and conditions of the Creative Commons Attribution (CC BY) license (<https://creativecommons.org/licenses/by/4.0/>).

1. Introduction

Joining metals and ceramics to combine the advantages of both material classes has been attractive for many engineering applications. SiC is a ceramic typically employed for joining with metals because of its high strength, extraordinary hardness, thermal properties, and electrical conductivity. The combination of SiC with light alloys such as Al alloys, exhibits potential engineering applications [1].

There has been considerable research on joining between SiC and steels [2–6] or nickel-based alloys [7–9]; however, surprisingly, there have been only a few reports in the literature on joining between SiC and Al alloys [1,10–12]. This may be due to the inherent technical difficulty of achieving good bonding between SiC and Al alloys.

First, because of the low melting point of Al alloys (typically below 660 °C), it is difficult to braze Al alloys and SiC using copper- or silver-based active filler materials [13,14], whose melting points are usually above those of Al alloys. Teng et al. [12] reported a brazing process using an Al₂₀Cu₆SiNiMg filler alloy to achieve the bonding of aluminum alloy 2219 to a pre-metalized SiC, but the maximum shear strength of the joints was low, at 16 MPa only.

Second, it is difficult to join Al alloys to SiC through the melting of the alloys because the wettability between molten Al alloys and SiC is usually poor [15]. Sozhamannan et al. studied the effect of temperature around 700 °C to 900 °C on the Al/SiC interfacial bonding but achieved a very low bonding strength (<0.5 MPa) in both Al6061/SiC joints [10] and Al-11Si/SiC joints [11].

Third, another major issue is the large mismatch of the coefficient of thermal expansion (CTE) between Al alloys and SiC. The large mismatch in the CTE may result in high residual stresses between the two dissimilar materials and lead to a low strength of the joints [16].

With the increasingly widespread use of ceramic particulate-reinforced aluminum matrix composites in automotive and other industries, many studies have been carried out on the wetting behavior and interfacial reactions of Al/SiC system [15,17–19]. Cong et al. [17] reported that the wettability of Al/SiC at 1000 °C was improved with the addition of 7 wt.% (weight percentage) and 12 wt.% Si in Al melt. Huang et al. [19] observed that the contact angle of Al/SiC at 1050 °C decreased considerably from 62° to 23° when the Si content increased from 4.8 at.% (atomic percentage) to 29.2 at.%. The addition of the Si element in Al alloys is generally found to help improve the wettability of Al/SiC at high temperatures (1000 °C or above). Therefore, it is possible to improve the bonding strength of Al/SiC by adding large amounts of Si to Al alloys.

Moreover, when the Si content in aluminum alloys increases to very high levels (e.g., 30 wt.% or more), the CTE of the alloys decreases significantly [20,21]. This helps reduce the mismatch in the CTE in the Al/SiC joint. However, to the best of the authors' knowledge, no papers have been published studying dissimilar material joining between Al and SiC using high-Si Al alloys.

In the current research, four types of Al alloys with different Si contents (7 wt.%, 12 wt.%, 30 wt.%, and 50 wt.%) were explored for pressure-less bonding with SiC at high temperature. The study has succeeded in producing strong Al/SiC joints through the use of high-Si alloys. The shear strength achieved (28.8 MPa) is far higher than those reported previously by Teng et al. (16 MPa) [12] and by Sozhamannan et al. (<0.5 MPa) [10,11].

2. Materials and Methods

Four types of Al alloys with varying Si contents were used for the study of dissimilar material joining between SiC and Al alloys. The SiC was purchased from Kaihongfei Electronic Co., Ltd., Guangzhou, China. The A356 and Al4047 alloys were purchased from SL Metal Pte Ltd., Singapore, and Jiaming Boye Non-ferrous Metals Ltd., Beijing, China, respectively. The high-Si Al alloys (Al-30Si and Al-50Si) were prepared by casting using high-purity Al (99.9%) and Si (99.9%). The chemical compositions of the Al alloys are shown in Table 1.

Table 1. Chemical compositions of the Al alloys used in this study (wt.%).

Al Type	Al	Si	Fe	Cu	Mg	Zn	Mn	Ni
A356	balance	7	0.2	0.2	0.3	0.1	0.1	-
Al4047	balance	12	0.3	0.8	1.0	-	0.1	0.8
Al-30Si	balance	30	≤0.1	-	-	-	-	-
Al-50Si	balance	50	≤0.1	-	-	-	-	-

The Al alloys and SiC blocks were ground using SiC paper and resin-bonded diamond, respectively, and then cleaned in an ultrasonic bath prior to the joining process. The dissimilar material joining process was carried out in a vacuum tube furnace (Lenton, Hope Valley, UK) under a vacuum pressure of 10^{-4} mBar. The Al alloys of 0.7 g in weight were melted onto SiC blocks with 10 mm × 10 mm × 10 mm dimensions at a temperature of 1100 °C, as shown in Figure 1. The heating rate was set at 5 °C·min⁻¹, and the holding time at 1100 °C was 30 min. The samples were cooled down to room temperature in the vacuum furnace.

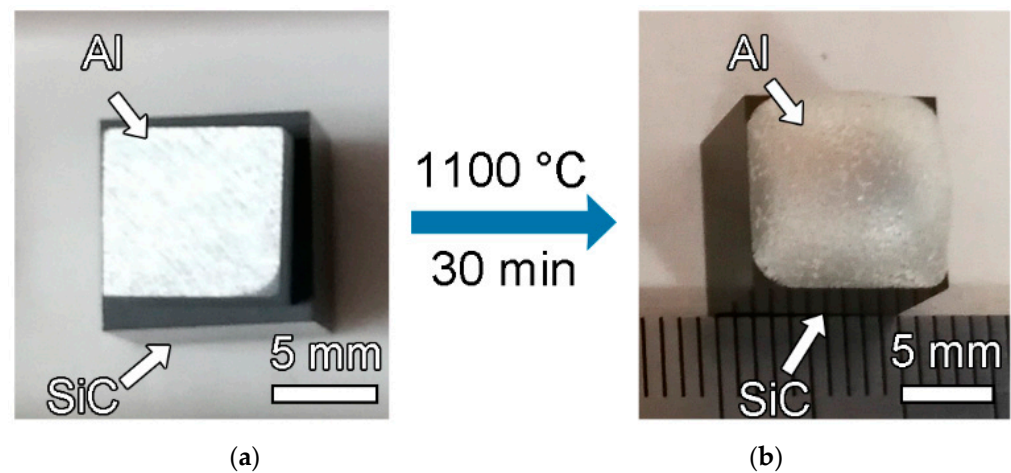


Figure 1. Photos showing (a) placement of 0.7 g Al alloy on SiC block before heating and (b) the sample after the completion of the bonding process.

A JEOL-7600 field emission scanning electron microscope (SEM; JEOL, Tokyo, Japan) was used to observe the microstructures of the Al/SiC joints. The interfacial reaction products were identified by energy dispersive spectroscopy (EDS; Oxford Instruments, Abingdon, UK) and X-ray diffraction (XRD; Panalytical Empyrean, Malvern, UK).

Shear tests were conducted on an Instron-5569 universal testing system (Instron, Norwood, MA, USA) at room temperature using displacement control at a fixed rate of $0.5 \text{ mm}\cdot\text{min}^{-1}$ [22]. Figure 2 shows the in-house designed jig used for the shear test. For each type of Al/SiC joint, at least three samples were tested to obtain an average bonding strength.

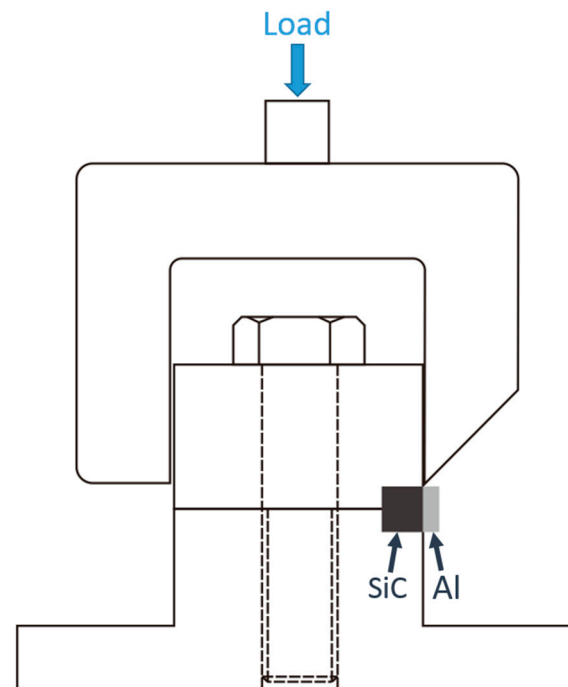


Figure 2. Schematic graph of the shear test jig.

3. Results and Discussion

3.1. Effect of Si Content on Bonding Strength

The shear fracture loads were low for the joints between SiC and the two types of Al alloys with low Si contents (i.e., A356 and Al4047) but became considerably higher for the joints between SiC and the two high-Si Al alloys (i.e., Al-30Si and Al-50Si). Typical load–

displacement curves of different Al/SiC joints are shown in Figure 3a–d and compared in Figure 3e.

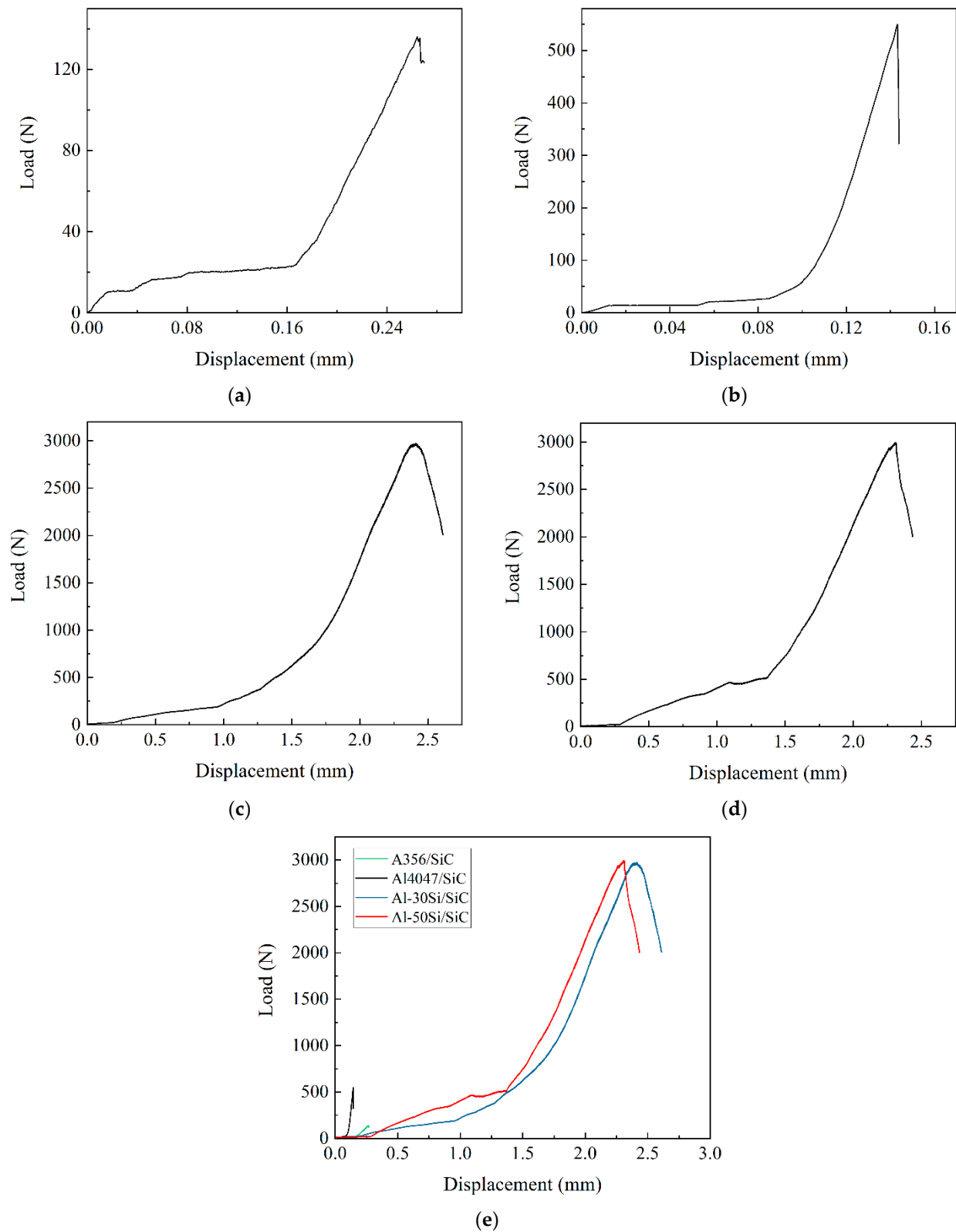


Figure 3. Typical load–displacement curve of (a) A356/SiC joint, (b) Al4047/SiC joint, (c) Al-30Si/SiC joint, and (d) Al-50Si/SiC joint; (e) comparison of the load–displacement curves of the four different Al/SiC joints.

The bonding strengths were calculated as the maximum load from the load–displacement curve divided by the bonding surface area and are shown in Figure 4 as a function of the Si content. The bonding strengths between SiC and the low-Si alloys were low, at 1.9 MPa for A356/SiC and 3 MPa for Al4047/SiC. It is clearly seen that the bonding strength of Al/SiC improved remarkably with the increase in Si content in Al alloys. The maximum bonding strength of 28.8 MPa was achieved for the Al-30Si/SiC joint. It is noted that this value was about 15 times higher than that of the Al A356/SiC joint. The bonding strength of the joint with the higher Si content alloy (i.e., Al-50Si) did not show further improvement.

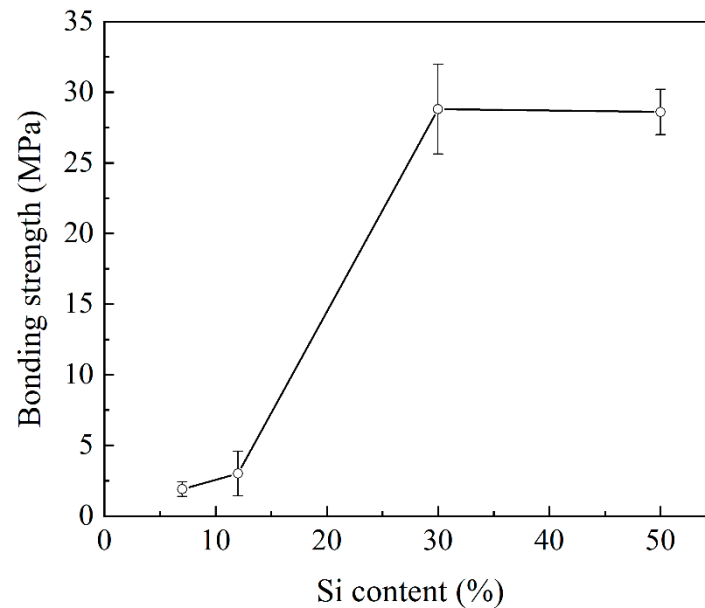


Figure 4. Plot showing the effect of Si content on the bonding strength of the Al/SiC joint (error bar represents standard deviation in tested samples).

3.2. Effect of Si Content on CTE

Table 2 compares the CTE values of the materials used in this study. The CTE of the Al alloys is much higher than that of SiC. This difference in the CTE would naturally generate thermal stresses in the Al/SiC joints that could cause cracking in the joints and, consequently, lower the bonding strength [16].

Table 2. CTE values of the materials.

Materials	Si Content (wt.%)	CTE ($\times 10^{-6} \text{ K}^{-1}$)	Refs.
SiC	-	4.7	[12]
A356	7	21.4	[23]
Al4047	12	19.4	[23]
Al-30Si	30	14~16	[24]
Al-50Si	50	10~12	[25]

It can be noted from Table 2 that the CTE tends to decrease with increasing Si content in the Al alloys. The CTE values for A356 and Al4047 are about $20 \times 10^{-6} \text{ K}^{-1}$. With the increase in Si content to 30 wt.%, the CTE value for the Al-30Si alloy is reduced to about $15 \times 10^{-6} \text{ K}^{-1}$. The 25% reduction in the CTE value is significant, and the reduction in the CTE mismatch may contribute to the improvement in the bonding strength. However, it should be noted that the CTE value for the Al-50Si alloy is further reduced by about one-third compared with that of the Al-30Si alloy, but the bonding strength was not further improved (Figure 4). It can be deduced from the analyses that the reduction in the CTE mismatch contributes to the improvement in bonding strength, but there may be more important factors influencing the bonding strength.

3.3. Effect of Si Content on Interfacial Reactions

To illustrate the effect of Si content on the interfacial microstructure, one joint between SiC and low-Si Al alloy (Al4047/SiC) and one joint between SiC and high-Si Al alloy (Al-50Si/SiC) were chosen. The backscattered electron SEM image of the Al4047/SiC interface is shown in Figure 5a. A clear reaction layer with a thickness of a few micrometers could be seen at the interface, and several cracks as marked by arrows were observed in this reaction layer.

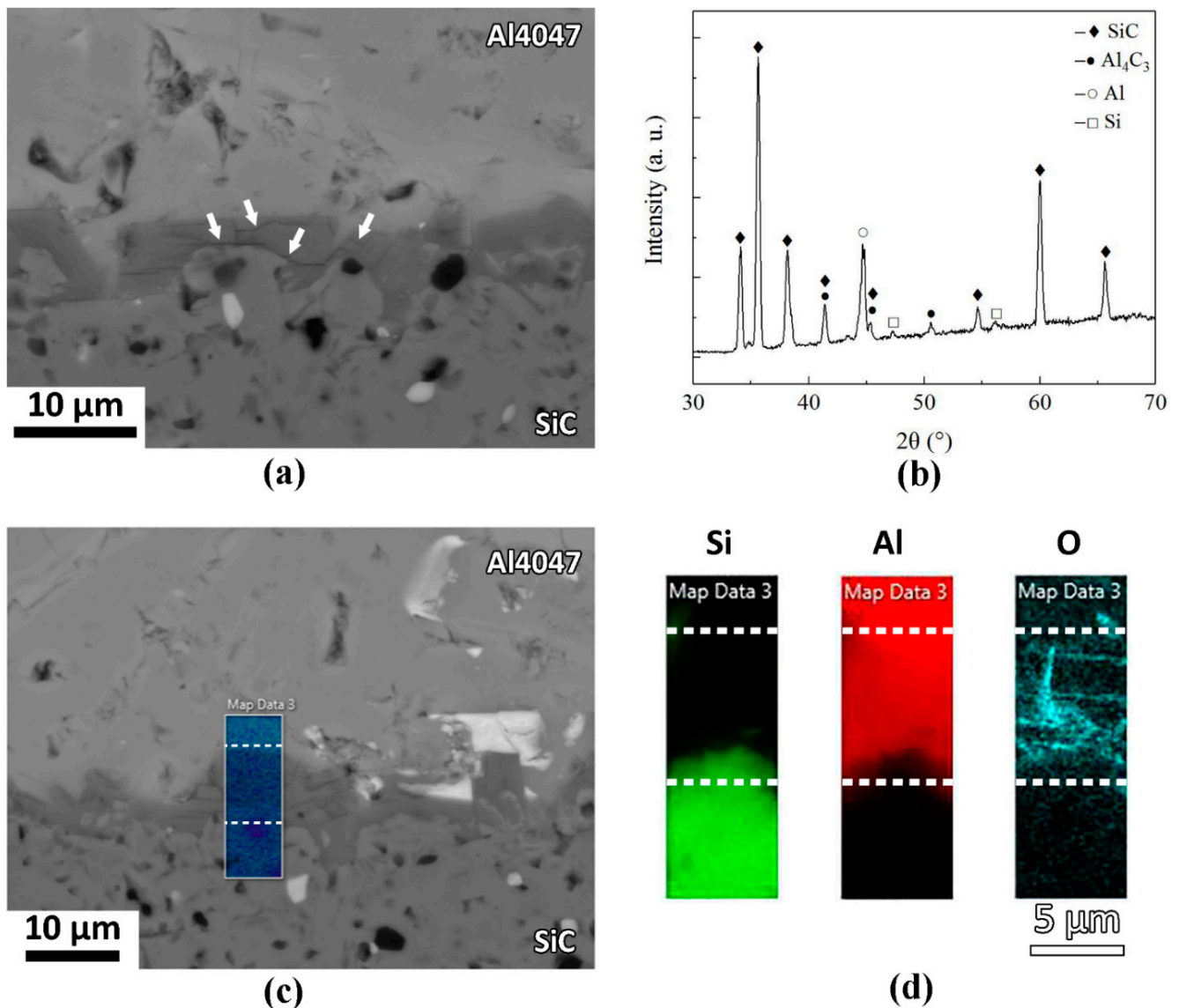


Figure 5. (a) Backscattered electron micrograph of Al4047/SiC joint showing interfacial layer and microcracks (arrowed) in the layer; (b) XRD pattern of Al4047/SiC joint; (c) SEM image showing the rectangular area for EDS in the Al4047/SiC joint; and (d) corresponding EDS mapping results of the area in (c). (The white dashed lines denote the reaction layer in the interfacial area).

The XRD patterns (Figure 5b) show some peaks belonging to Al₄C₃ phase formed at the interface of Al4047/SiC. Given the relatively small volume fraction of interfacial products, it is understandably difficult to identify by conventional XRD in terms of the detection limit of the peak intensity. In addition, some Al₄C₃ peaks overlapped with other peaks from the SiC substrates, as shown in the XRD data in Figure 5b. The occurrence of Al₄C₃ peaks at the given 2-theta positions in the XRD spectrum was also reported by Ma et al. [26].

Figure 5c,d show the EDS elemental mapping results at the interface. This reaction layer consisted mostly of Al along with Si and O. A high concentration of oxygen at the interface was noted. The high oxygen concentration could be linked to the formation of Al_2O_3 during the heating stage and its retention at the interface through the cooling cycle. The hexagonal Al_4C_3 structure has a high c/a ratio of ~ 7.48 and would thus be more prone to delamination, in this case, by solidification stresses predominantly along the slender crystallographic c-axis. This would imply that the observed cracks were along the basal planes of the carbides wherein local O attack consequently occurred (Figure 5d).

In contrast to the results of the observation of the Al4047/SiC interface, there was no obvious reaction layer at the Al-50Si/SiC interface, and no Al_4C_3 was detected, as shown in Figure 6.

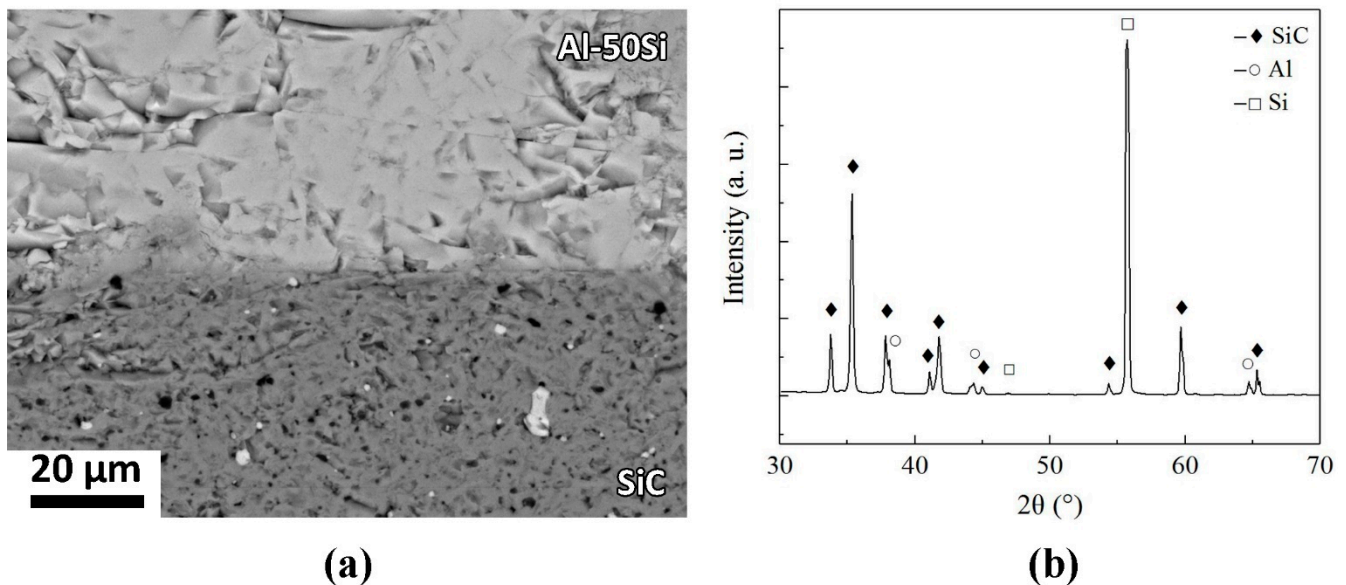


Figure 6. (a) Backscattered electron micrograph of Al-50Si/SiC joint showing no obvious interfacial reaction layer or microcracks; (b) XRD pattern of Al-50Si/SiC joint.

The formation of Al_4C_3 has been reported in SiC-reinforced aluminum composites produced by stir casting [27] through the following reaction:



During the heating stage, the reaction starts occurring above the melting point of Al, and SiC also becomes unstable in the meantime [28]. When the Al alloys completely melt with continued heating, changes arising from the reaction of SiC with the liquid phase are observed in the system until an equilibrium Si concentration in Al melt is attained. At 1100 °C, this equilibrium concentration is approximately 18 wt.% Si [29], below which Al alloys react with SiC to form Al_4C_3 , as was the case in the Al4047/SiC (12 wt.% Si) joint.

The reaction between Al and SiC is believed to be necessary to achieve the metal/ceramic bonding, but the kinetics and the extent of the interfacial reaction can vary under different conditions. Above the equilibrium concentration, such as in Al-50Si wherein the liquid Al phase has a 50 wt.% Si concentration, the reverse of reaction occurs between the alloy and the already-formed Al_4C_3 , resulting in SiC and Al formation.

Besides this reaction, particularly in the low-Si Al alloys (Al4047 and A356), the dissolution of C from SiC would take place, causing further nucleation of Al_4C_3 precipitates in the liquid Al [30]. However, because of the presence of high Si content in the liquid melt (Al-30Si and Al-50Si), the C-solubility is also dramatically reduced, thereby preventing the formation of the brittle carbide phase.

The low bonding strength of the joints between SiC and low-Si Al alloys is mainly attributed to the brittleness of Al_4C_3 carbide, which is evident from the presence of cracks within the phase. On the other hand, the presence of the thin Al-rich metallic film at the interface of the joints by the suppression of the brittle Al_4C_3 phase is also believed to be responsible for the improved strength of the metal/ceramic joints.

3.4. Perspectives

Due to the excellent mechanical properties of the joint, high-Si Al alloys have the potential to be used to bond with SiC. This could be effective in solving the poor wetting problem and reducing the large thermal stresses between Al and SiC. Moreover, this method provides an alternative strategy to achieve easier bonding of SiC with other types of Al alloys subsequently, as shown in Figure 7. The filler materials could be Zn-based, Sn-based, or Cu interlayers, which have been successfully used for brazing high-Si Al alloys [31–35].

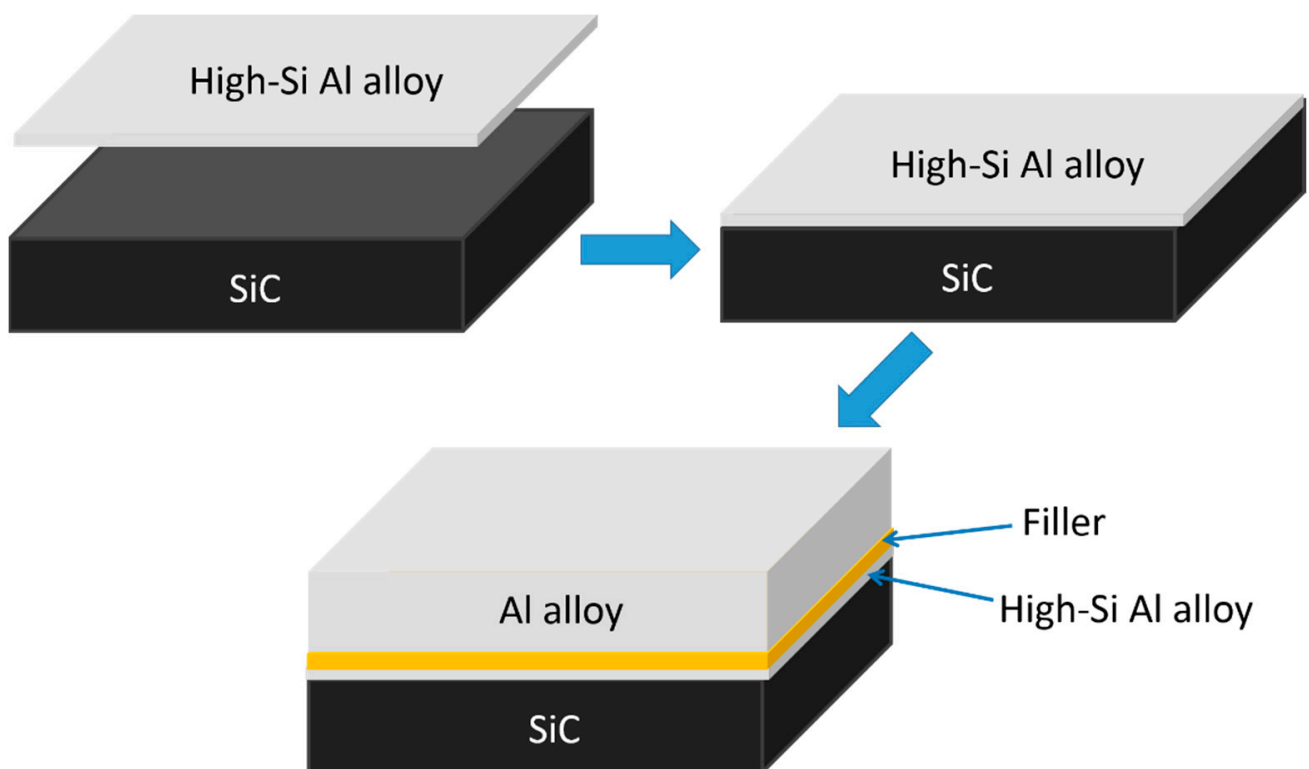


Figure 7. Illustration of the strategy for joining between SiC and a wide range of Al alloys through use of high-Si Al alloys.

It is noted that the melting point of the Al-50Si alloy is 1050 °C according to the Al-Si binary phase diagram, and the bonding temperature used in this study was 1100 °C. With the addition of more Si, the melting point of the Al-Si alloys increases. High-Si Al alloys with over 50 wt.% Si may not melt or achieve good bonding with SiC at 1100 °C. Therefore, no Al alloy with Si content higher than 50 wt.% was tested in the current study. It would be interesting to carry out further research to study the bonding behavior of high-Si Al alloys with more than 50 wt.% Si or 18–30 wt.% Si at various bonding temperatures to find the optimum parameters for bonding with SiC.

4. Conclusions

In this study, dissimilar material joining between SiC and Al was carried out successfully using Al alloys with varying Si contents (7–50 wt.%) through a pressure-less bonding process. The mechanical properties and microstructures of the joints were characterized. The main conclusions are as follows:

- (1) The bonding strength of the joints was low when using low-Si Al alloys (A356 and Al4047) to bond with SiC. A significant improvement in bonding strength was found in high-Si Al/SiC joints (Al-30Si/SiC and Al-50Si/SiC).
- (2) Microstructure characterization revealed that a reaction layer with a thickness of a few micrometers occurred at the interface in the Al4047/SiC joint. The reaction layer consisted of brittle Al₄C₃ phase, resulting in a lower bonding strength of the joints.
- (3) The remarkable improvement in bonding strength in high-Si Al/SiC joints could be attributed to the reduced thermal stresses and the suppression of brittle reaction products at the interface.

Author Contributions: Conceptualization, W.Z. and Y.Y.; methodology, W.Z. and Y.Y.; validation, W.Z. and Z.D.; formal analysis, W.Z., Y.Y. and A.B.; investigation, Y.Y., A.B., J.L.T. and Z.D.; data curation, Y.Y. and A.B.; writing—original draft preparation, Y.Y. and A.B.; writing—review and editing, Y.Y., A.B. and W.Z.; visualization, Y.Y. and A.B.; supervision, W.Z.; project administration, W.Z. and Z.D.; funding acquisition, W.Z. and Z.D. All authors have read and agreed to the published version of the manuscript.

Funding: This research was funded by the Ministry of Defence (MINDEF), Singapore, through grant #001498-00008.

Institutional Review Board Statement: Not applicable.

Informed Consent Statement: Not applicable.

Data Availability Statement: Not applicable.

Acknowledgments: The authors would like to thank Jianming Yuan of Temasek Laboratories at NTU for his advice and research support.

Conflicts of Interest: The authors declare no conflict of interest.

References

1. Lin, Y.C.; McGinn, P.J.; Mukasyan, A.S. High temperature rapid reactive joining of dissimilar materials: Silicon carbide to an aluminum alloy. *J. Eur. Ceram. Soc.* **2012**, *32*, 3809–3818. [[CrossRef](#)]
2. Südmeyer, I.; Hettesheimer, T.; Rohde, M. On the shear strength of laser brazed SiC-steel joints: Effects of braze metal fillers and surface patterning. *Ceram. Int.* **2010**, *36*, 1083–1090. [[CrossRef](#)]
3. Zhong, Z.; Hinoki, T.; Jung, H.C.; Park, Y.H.; Kohyama, A. Microstructure and mechanical properties of diffusion bonded SiC/steel joint using W/Ni interlayer. *Mater. Des.* **2010**, *31*, 1070–1076. [[CrossRef](#)]
4. Zhong, Z.; Hinoki, T.; Kohyama, A. Microstructure and mechanical strength of diffusion bonded joints between silicon carbide and F82H steel. *J. Nucl. Mater.* **2011**, *417*, 395–399. [[CrossRef](#)]
5. Zhu, M.; Chung, D.D.L. Active brazing alloy containing carbon fibers for metal-ceramic joining. *J. Am. Ceram. Soc.* **1994**, *77*, 2712–2720. [[CrossRef](#)]
6. Huang, B.; Shu, Z.; Li, T.; Li, H.; Zhang, D.; Yi, F. Effect of different interlayers on microstructure and mechanical properties of diffusion-bonded joints between SiC and 316LN. *Philos. Mag.* **2022**, *102*, 137–152. [[CrossRef](#)]
7. Song, Y.; Liu, D.; Song, X.; Hu, S.; Cao, J. In-situ synthesis of TiC nanoparticles during joining of SiC ceramic and GH99 superalloy. *J. Am. Ceram. Soc.* **2019**, *102*, 6529–6541. [[CrossRef](#)]
8. Xiong, H.P.; Mao, W.; Xie, Y.H.; Guo, W.L.; Li, X.H.; Cheng, Y.Y. Brazing of SiC to a wrought nickel-based superalloy using CoFeNi(Si, B)CrTi filler metal. *Mater. Lett.* **2007**, *61*, 4662–4665. [[CrossRef](#)]
9. Shi, H.; Chai, Y.; Li, N.; Yan, J.; Peng, H.; Zhang, R.; Li, M.; Bai, D.; Chen, K.; Liu, Z.; et al. Investigation of interfacial reaction mechanism between SiC and Inconel 625 superalloy using thermodynamic calculation. *J. Eur. Ceram. Soc.* **2021**, *41*, 3960–3969. [[CrossRef](#)]
10. Sozhamannan, G.G.; Prabu, S.B. Evaluation of interface bonding strength of aluminum/silicon carbide. *Int. J. Adv. Manuf. Technol.* **2009**, *44*, 385–388. [[CrossRef](#)]
11. Sozhamannan, G.G.; Prabu, S.B. Influence of interface compounds on interface bonding characteristics of aluminium and silicon carbide. *Mater. Charact.* **2009**, *60*, 986–990. [[CrossRef](#)]
12. Teng, P.; Li, X.; Hua, P.; Liu, H.; Wang, G. Effect of metallization temperature on brazing joints of SiC ceramics and 2219 aluminum alloy. *Int. J. Appl. Ceram. Technol.* **2022**, *19*, 498–507. [[CrossRef](#)]
13. Xu, R.; Indacochea, J.E. Silicon nitride-stainless steel braze joining with an active filler metal. *J. Mater. Sci.* **1994**, *29*, 6287–6294. [[CrossRef](#)]
14. Bissig, V.; Galli, M.; Janczak-Rusch, J. Comparison of three different active filler metals used for brazing ceramic-to-ceramic and ceramic-to-metal. *Adv. Eng. Mater.* **2006**, *8*, 191–196. [[CrossRef](#)]
15. An, Q.; Cong, X.S.; Shen, P.; Jiang, Q.C. Roles of alloying elements in wetting of SiC by Al. *J. Alloys Compd.* **2019**, *784*, 1212–1220. [[CrossRef](#)]
16. Fernie, J.A.; Drew, R.A.L.; Knowles, K.M. Joining of engineering ceramics. *Int. Mater. Rev.* **2009**, *54*, 283–331. [[CrossRef](#)]

17. Cong, X.S.; Shen, P.; Wang, Y.; Jiang, Q. Wetting of polycrystalline SiC by molten Al and Al-Si alloys. *Appl. Surf. Sci.* **2014**, *317*, 140–146. [[CrossRef](#)]
18. Huang, Z.; Zhang, X.; Wang, T.; Liu, G.; Shao, H.; Wan, Y.; Qiao, G. Effects of Pd ion implantation and Si addition on wettability of Al/SiC system. *Surf. Coat. Technol.* **2018**, *335*, 198–204. [[CrossRef](#)]
19. Lee, J.C.; Park, S.B.; Seok, H.K.; Oh, C.S.; Lee, H.I. Prediction of Si contents to suppress the interfacial reaction in the SiCp/2014 Al composite. *Acta Mater.* **1998**, *46*, 2635–2643. [[CrossRef](#)]
20. Chien, C.W.; Lee, S.L.; Lin, J.C.; Jahn, M.T. Effects of Sip size and volume fraction on properties of Al/Sip composites. *Mater. Lett.* **2002**, *52*, 334–341. [[CrossRef](#)]
21. Bhowmik, A.; Yang, Y.; Zhou, W.; Chew, Y.; Bi, G. On the heterogeneous cooling rates in laser-clad Al-50Si alloy. *Surf. Coat. Technol.* **2021**, *408*, 126780. [[CrossRef](#)]
22. Fan, D.; Huang, J.; Wang, Y.; Chen, S.; Zhao, X. Active brazing of carbon fiber reinforced SiC composite and 304 stainless steel with Ti-Zr-Be. *Mater. Sci. Eng. A* **2014**, *617*, 66–72. [[CrossRef](#)]
23. Nunes, R.; Adams, J.H.; Ammons, M.; Avery, H.S.; Barnhurst, R.J.; Bean, J.C.; Beaudry, B.J. *Properties and Selection: Nonferrous Alloys and Special-Purpose Materials*; ASM International: Novelty, OH, USA, 1990; Volume 2, ISBN 978-1-62708-162-7.
24. Haque, A.; Shekhar, S.; Narayana Murty, S.V.S.; Ramkumar, J.; Kar, K.; Mondal, K. Fabrication of controlled expansion Al-Si composites by pressureless and spark plasma sintering. *Adv. Powder Technol.* **2018**, *29*, 3427–3439. [[CrossRef](#)]
25. Controlled Expansion (CE) Alloy Products—Sandvik Materials Technology. Available online: <https://www.materials.sandvik/en/products/ce-alloys/> (accessed on 12 October 2020).
26. Ma, B.; Wang, J.; Lee, T.H.; Dorris, S.E.; Wen, J.; Balachandran, U. Microstructural characterization of Al₄C₃ in aluminum–graphite composite prepared by electron-beam melting. *J. Mater. Sci.* **2018**, *53*, 10173–10180. [[CrossRef](#)]
27. Zhou, W.; Xu, Z.M. Casting of SiC reinforced metal matrix composites. *J. Mater. Process. Technol.* **1997**, *63*, 358–363. [[CrossRef](#)]
28. Iseki, T.; Maruyama, T.; Kameda, T. Interfacial reactions between SiC and aluminium during joining. *J. Mater. Sci.* **1984**, *19*, 1692–1698. [[CrossRef](#)]
29. Ferro, A.C.; Derby, B. Wetting behaviour in the Al-Si/SiC system: Interface reactions and solubility effects. *Acta Metall. Mater.* **1995**, *43*, 3061–3073. [[CrossRef](#)]
30. Viala, J.C.; Fortier, P.; Bouix, J. Stable and metastable phase equilibria in the chemical interaction between aluminium and silicon carbide. *J. Mater. Sci.* **1990**, *25*, 1842–1850. [[CrossRef](#)]
31. Zhu, L.; Wang, Q.; Shi, L.; Zhang, X.; Yang, T.; Yan, J.; Zhou, X.; Chen, S. Ultrarapid formation of multi-phase reinforced joints of hypereutectic Al-Si alloys via an ultrasound-induced liquid phase method using Sn-51In interlayer. *Mater. Sci. Eng. A* **2018**, *711*, 94–98. [[CrossRef](#)]
32. Wang, Q.; Zhu, L.; Chen, X.; Yan, J.; Xie, R.; Li, P.; Wang, Z.; Wang, Z.; Li, Y.; Zhou, X. Si particulate-reinforced Zn-Al based composites joints of hypereutectic Al-50Si alloys by ultrasonic-assisted soldering. *Mater. Des.* **2016**, *107*, 41–46. [[CrossRef](#)]
33. Wang, Q.; Chen, X.; Zhu, L.; Yan, J.; Lai, Z.; Zhao, P.; Bao, J.; Lv, G.; You, C.; Zhou, X.; et al. Rapid ultrasound-induced transient-liquid-phase bonding of Al-50Si alloys with Zn interlayer in air for electrical packaging application. *Ultrason. Sonochem.* **2017**, *34*, 947–952. [[CrossRef](#)] [[PubMed](#)]
34. Sun, Q.; Wang, H.; Yang, C. Microstructure and Properties of the Al-27Si/Cu/Al-50Si Joint Brazed by the Partial Transient Liquid Phase Bonding. *Metall. Mater. Trans. B Process Metall. Mater. Process. Sci.* **2018**, *49*, 933–938. [[CrossRef](#)]
35. Xu, L.; Wang, H.; Sun, Q.; Wan, W.; Chen, H. Effect of bonding temperature on microstructure and shear strength of the dissimilar Al/Al-27Si joints bonded by partial transient liquid phase bonding. *J. Manuf. Process.* **2019**, *41*, 297–306. [[CrossRef](#)]